DOI: 10.1002/chem.200901641

Supramolecular Architectures by Fullerene-Bridged Bis(permethyl-β-cyclodextrin)s with Porphyrins

Ying-Ming Zhang, Yong Chen, Yang Yang, Peng Liu, and Yu Liu*[a]

Abstract: The Hirsch–Bingel reaction of bis{4-methyl[1,2,3]triazolyl}malonic ester-bridged bis(permethyl-β-cyclodextrin) **1** with C_{60} has led to the formation of a new fullerene-bridged bis(permethyl-β-cyclodextrin) **2**, which has been comprehensively characterized by NMR spectroscopy, MALDI-MS, and elemental analysis. Taking advantage of the high affinity between **2** and 5,10,15,20-tetrakis(4-sulfonatophenyl)porphyrin (**3**) or [5,10,15,20-tetrakis(4-sulfonatophenyl)porphinato]zinc(II) (**4**), linear supramolecular architectures with a width of about 2 nm and a length ranging from hundreds of nanometers to micron dimension were conveniently constructed and fully investigated by transmission electron microscopy (TEM), atomic force microscopy (AFM), and scanning electron microscopy (SEM). Significantly, the photoinduced electron-transfer (PET) process between porphyrin and C_{60} moieties takes place within the **2**·**3** and **2**·**4** supramolecular architectures under light irradiation, leading to the highly efficient quenching of the porphyrin fluorescence. The PET process and the charge-separated state were investigated by means of fluorescence spectroscopy, fluorescence decay, cyclic voltammetry, and nanosecond transient absorption measurements.

Keywords: cyclodextrins · electron transfer · fullerenes · molecular assembly · photochemistry · porphyrinoids

Introduction

A photoinduced electron-transfer (PET) process is one in which electron transfer occurs when certain photoactive materials interact with light.[1] This phenomenon in donor–accepter (D–A) systems with unique photophysical and electrochemical properties, which are critical for engineering molecular electronics and optoelectronics, can mimic the process of photosynthesis artificially and open potential applications in the realization of the photovoltaic devices[2] and solar cells with high efficiency.[3] As a result, considerable effort has been devoted to the development of covalently linked donor–acceptor systems in recent years. However, compared to the covalent method, it is a challenging topic to control the self-assembly of elaborately designed non-covalent supramolecular systems with PET capability for interdisciplinary research in the fields of chemistry, biology, and materials science. There are two principle aspects to illuminate the advantages and significance in the design of supramolecular multichromophoric arrays displaying directional energy and electron transfer. Firstly, it is widely known that nature relies on supramolecular methodology to achieve self-assembly. Most of photosynthetic reactions occur in the water environment and the whole complex array of components is spatially defined with weak noncovalent interactions that suffice to mediate the energy- or electron-transfer process. The convenience and diversity of synthesis is the second aspect. The covalently linked system is a difficult and one-off process, because the assembly of the molecule is irreversible once it is formed. It is not usually possible to undo the components and reassemble them in a different way. Taking advantage of supramolecular chemistry to assemble photoactive complexes, one can control the molecular arrangements precisely at the supramolecular level to get well-defined nanoscopic architectures with long-lived charge-separated states and modulate the spatiotemporal change between both electroactive entities, which would not be accessible in intramolecular PET process.[4]

[a] Y.-M. Zhang, Dr. Y. Chen, Y. Yang, P. Liu, Prof. Dr. Y. Liu
Department of Chemistry
State Key Laboratory of Elemento-Organic Chemistry
Nankai University, Tianjin, 300071 (P. R. China)
Fax: (+86) 22-23503625
E-mail: yuliu@nankai.edu.cn

Supporting information for this article is available on the WWW under http://dx.doi.org/10.1002/chem.200901641. It contains a Job's plot, UV/Vis titration spectra, fluorescence emission changes, fluorescence decay profiles, transient absorption spectra, and 2D NOESY spectrum of the **2**·**3** system.

Among the wide variety of donor–acceptor systems, the fullerene and porphyrin derivatives are attractive and promising candidates in the light of the photoinduced intermolecular electron transfer and extensively studied in this field. Although numerous covalent[5] or noncovalent[6] multicomponent synthetic donor–accepter molecules, polymeric composite materials,[7] and conjugated polymers[8] for efficient photoinduced electron transfer process have been investigated, studies on the photoinduced transport of electrons in nanoscale ordered materials with specific shape and novel functionalities mediated by the equidistant and regular host–guest complexation as donor and accepters to achieve linear self-assemblies in aqueous media are still rare, to the best of our knowledge. Herein, we adopt a molecular recognition strategy and supramolecular nanotechnology to construct the ordered fullerene–porphyrin supramolecular architectures with a linear array through the complexation of fullerene-bridged bis(permethyl-β-cyclodextrin)s with porphyrin derivatives (Scheme 1). In addition, their complexation mode and photoinduced electron-transfer behavior in water were also investigated by UV/Vis spectroscopy, fluorescence spectroscopy, fluorescence decay, cyclic voltammetry, and nanosecond transient absorption measurements, which will help us understand this important, but less investigated, area of supramolecular chemistry.

Results and Discussion

Synthesis: The reaction between mono(6-deoxy-6-azido)-permethyl-β-CD and propargyl malonate in THF/H_2O afforded **1** through "click chemistry" (Scheme 1) in 70% yield. Then, **1** underwent a Hirsch–Bingel reaction with C_{60} in toluene/DMF to yield fullerene bridged bis(permethyl-β-CD) **2** in 37% yield. Benefiting from the good solubilization ability of permenthyl-β-CD units, **2** showed a satisfactory solubility up to 1 mM in water. Through the very strong binding of permenthyl-β-CD cavity with porphyrin derivatives reported by Kano and co-workers[9] the linear supramolecular nanoarchitectures could be constructed by the association of **2** with **3** and **4** in aqueous solution and were sufficiently characterized by UV/Vis, fluorescence spectrosco-

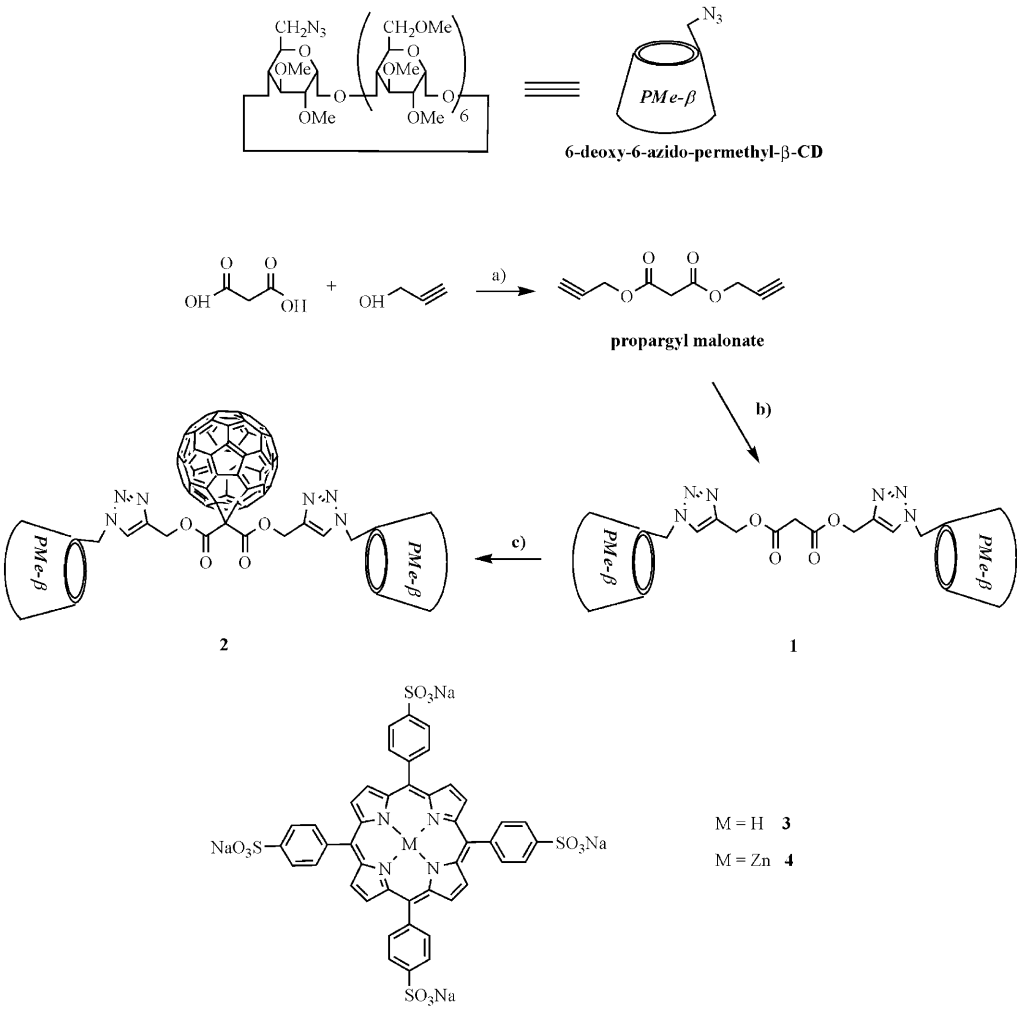

Scheme 1. Syntheses of **1** and **2** and molecular structures of porphyrin derivatives **3** and **4**. Reagents and conditions: a) *p*-toluenesulfonic acid, benzene, 120°C; b) mono(6-deoxy-6-azido)-permethyl-β-CD (3 equiv), sodium ascorbate, $CuSO_4 \cdot 5H_2O$, THF/H_2O; c) C_{60} (1 equiv), CBr_4, DBU, toluene/DMF.

py, fluorescence decay spectroscopy, cyclic voltammetry, nanosecond transient spectroscopy, transmission electron microscopy (TEM), atomic force microscopy (AFM) and scanning electron microscopy (SEM).

UV/Vis spectroscopy: As seen from Figure 1, the UV/Vis spectrum of **1** showed a weak absorption band of triazole group around 270 nm. In the UV/Vis spectrum of **2**, two new absorption bands, which were assigned to the C_{60} moiety, appeared at 259 and 329 nm. This information,

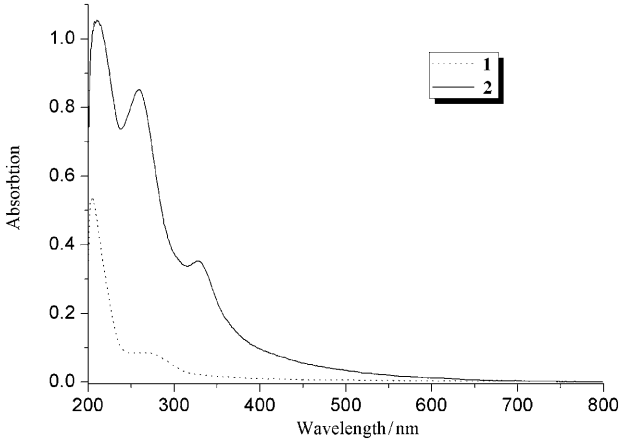

Figure 1. UV/Vis spectra of **1** (10 μM), **2** (10 μM) recorded in ethanol–phosphate buffer (v/v = 1:4, pH 7.2) at room temperature.

along with the NMR spectroscopy, MS, and elemental analysis results, jointly confirmed the incorporation of C_{60} into **1**. Moreover, the UV/Vis spectrum of **2** showed no maximum at 430 nm, which may indicate aggregation of the C_{60} moiety in **2** to some extent.[10] Quantitative investigation of the inclusion complexation behaviors of **2** with **3** and **4** were examined in ethanol–phosphate buffer (v/v = 1:4, pH 7.2) solution by means of UV/Vis spectroscopy titration. As seen from Figure 2 (bottom), the Soret band of **4** (and **3** in Figure S2 in the Supporting Information) dramatically changed with the addition of **2**, accompanied by the appearance of an isosbestic point at 424 nm (and 417 nm for **3**), which indicated the simple one-step transformation from the free **2** to the **4**-associated (and **3**-associated) species. The curve of $\Delta A_{2\text{-}4}$ ($\Delta A_{2\text{-}4} = \Delta A_{2+4} - \Delta A_4$, A_4 was defined as the absorption intensity of **4** at 422.5 and 424.8 nm, respectively) versus the **2**/**4** molar ratio showed an inflexion point at a molar ratio of 1 (Figure 2 top), corresponding to a 1:1 complexation stoichiometry between **2** and **4**. This result was further confirmed by Job's plot, which showed a maximum peak at a molar fraction of 0.5 (Figure S1 in the Supporting Information). Moreover, no other evident new peaks were found in UV/Vis spectrum of **2**·**4** system, indicating that the accepter **2** and donor **4** components did not interact with each other in the ground state.[11] In addition, the complex stability constants (K_s) between **2** and the porphyrin derivatives were calculated as $9.03\times10^5\,M^{-1}$ for **2**·**3** and $8.98\times10^5\,M^{-1}$ for **2**·**4**

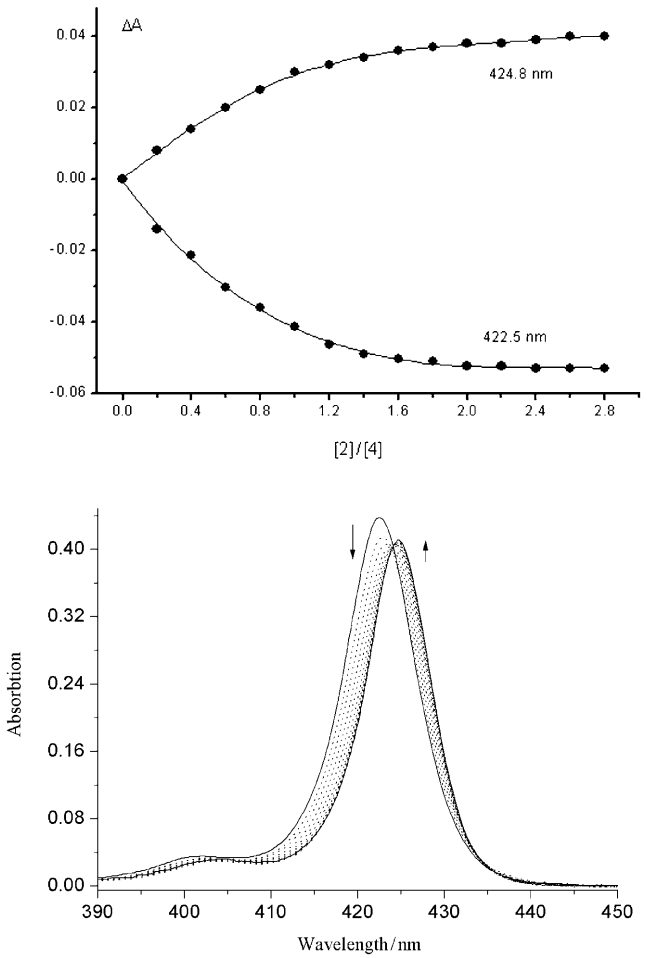

Figure 2. Bottom: UV/Vis titration spectra of **4** (1.01 μM) upon addition of **2** (0-2.76 μM) in ethanol–water–phosphate buffer (v/v = 1:4, pH 7.2), for which a solution of **2** in the same concentration (0–2.76 μM) was used as a reference. Top: the absorption change (ΔA) vs. **2**/**4** molar ratio recorded at $\lambda = 422.5$ and 424.8 nm, respectively.

by analyzing the sequential changes of the absorbtion intensity at varying host concentrations and by using the Hildebrand–Benesi equation.[12] In repeated measurements, the K_s values were reproducible within an error of ±5%.

Fluorescence spectroscopy: As illustrated in Figure 3, approximately 96% of the fluorescence intensity of **4** decreased with the stepwise addition of **2**, accompanied by a hypsochromic shift of the emission peak of **4** (from 604 nm to 598 nm). In the control experiment, the emission intensity of **4** enhanced with an increase concentration of **1** or permethyl β-CD and was attributed to the hydrophobic nature of CD cavity to decrease the collisional quenching of free porphyrins.[9a,10] Considering the fullerene and porphyrin are good donor and acceptor molecules, respectively,[13] these results indicated that there should be a PET process from the excited singlet state of porphyrin to the C_{60} moiety of **2** in solution, which was further confirmed by fluorescence decay spectroscopy, cyclic voltammetry, and nanosecond transient absorption spectroscopy as described below.

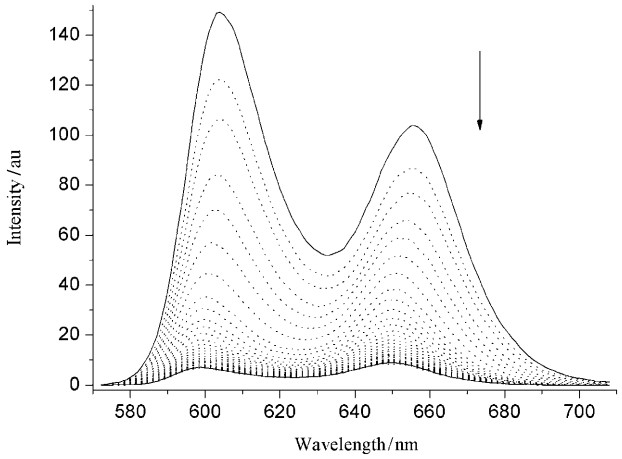

Figure 3. Fluorescence emission changes of **4** (1.00 μM) upon addition of **2** (0–4.44 μM from top to bottom) recorded in ethanol–water–phosphate buffer (v/v = 1:4, pH 7.2) (λ_{ex} = 422 nm).

Fluorescence decay spectroscopy: Fluorescence decay experiments were carried out in order to investigate the PET process quantitatively. Prior to the addition of **2**, the fluorescence decay curve of **3** and **4** was mono-exponential, from which the lifetimes of 11.95 (100%) and 2.07 ns (100%) were determined, respectively. The lifetimes prolonged to 13.42 (100%) and 2.38 ns (100%), when **1** or permethyl β-CD was added to the solution (Figure 4). These observations indicated that the CD cavity could protect the porphyrin from fluorescence quenching to some extent. In sharp contrast, after the addition of **2**, the fluorescence decay curve became double-exponential, and gave two lifetimes at 0.75 (82.8%) and 2.34 ns (17.2%) for **2·4**. In the case of **2·3**, two lifetimes at 2.08 (70.7%) and 8.94 ns (29.3%) were obtained. Although the detailed mechanism is not very clear, these results are basically consistent with reported observations of the PET process between CD-modified multiwalled carbon nanotubes and porphyrin derivatives.[14] The shorter lifetime might correspond to the electron-transfer quenching between the encapsulated porphyrin and the appended C_{60} moiety out of CD cavity. The rates of charge separation (k_{CS}^S) and the quantum yields (Φ_{CS}^S) of electron transfer reactions was evaluated by using Equations (1) and (2), respectively. In these equations $\tau_{F(complex)}$ is the fluorescence lifetime of the short-lived components, and $\tau_{F(ref)}$ is the fluorescence lifetime of **3** or **4**. Thus, the k_{CS}^S values were obtained as $4.06\times10^8\ s^{-1}$ for **2·3** and $9.06\times10^8\ s^{-1}$ for **2·4**. Correspondingly, the Φ_{CS}^S values were evaluated as 0.85 for **2·3** and 0.68 for **2·4** (Table 1).

$$k_{cs}^{s} = 1/\tau_{F(complex)} - 1/\tau_{F(ref)} \quad (1)$$

$$\Phi_{CS}^{S} = [(1/\tau_{F(complex)}) - (1/\tau_{F(ref)}]/(1/\tau_{F(complex)}) \quad (2)$$

Table 1. The fluorescence lifetimes and relative quantum yields of **3** and **4** in the absence and presence of permethyl-β-CD, **1** and **2** and the corresponding rates of charge separation (k_{CS}^S) and the quantum yields (Φ_{CS}^S) of **2·3** and **2·4**.

Guest	Host	τ_1 [ns]	Φ [%]	τ_2 [ns]	Φ [%]	k_{CS}^S [s^{-1}]	Φ_{CS}^S
3		11.95	100				
3	permethyl-β-CD	13.42	100				
3	**1**	13.42	100				
3	**2**	2.08	70.7	8.94	29.3	4.06×10^8	0.85
4		2.07	100				
4	permethyl-β-CD	2.38	100				
4	**1**	2.38	100				
4	**2**	0.75	82.8	2.34	17.2	9.06×10^8	0.68

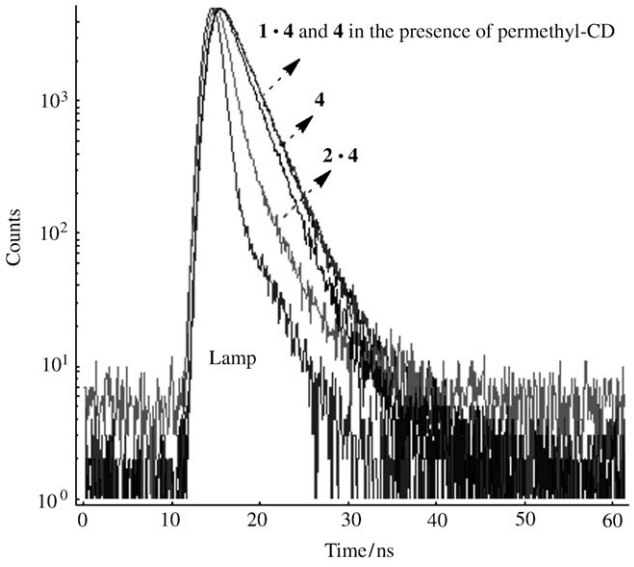

Figure 4. Fluorescence decay profiles of **4** (0.99 μM), **4** (0.99 μM) in the presence of **1** (3.42 μM), **4** (0.99 μM) in the presence of **2** (3.36 μM), and **4** (0.99 μM) in the presence of permethyl-β-CD (11.70 μM) in ethanol–water–phosphate buffer (v/v = 1:4, pH 7.2) at λ = 603 nm (λ_{ex} = 422 nm).

It is significant to compare the results reported earlier for the covalently linked dyads bearing C_{60} and porphyrin moieties in organic solvents with the supramolecular dyads of the present study. Although the molecular flexibility of the non-covalently systems appeared to accelerate the charge-recombination, the highly efficient photoinduced electron transfer in supramolecular dyads was successfully achieved through the strong complexation interactions, especially in water.

Electrochemical studies: As an interesting class of electroactive materials to probe the photoinduced intra/intermolecular electron transfer, fullerene derivatives are good electron acceptors forming charge-transfer complexes with porphyrin.[15] Herein, the cyclic voltammetry experiments were carried out to investigate the existence of charge-transfer interactions between the donor and the acceptor and also to evaluate the energetics of electron-transfer reactions. The electrochemical behaviors of **2** and **3** were investigated in dry THF and aqueous solution, with $(tC_4H_9)_4NClO_4$ and NaCl as the supporting electrolyte, respectively. The experi-

ments were performed with a wide potential window in order to obtain a thorough characterization of the redox process. Furthermore, the Rehm–Weller equation [Eq. (3)] was introduced to estimate the Gibbs free energy (ΔG_{cs}) of an electron-transfer reaction.

$$\Delta G_{cs} = e(E_{ox} - E_{red}) - E_{00} - e^2/\varepsilon d \quad (3)$$

In Equation (3) E_{00} is the excited singlet energies of porphyrins, e is the electron charge in Coulomb, d is the distance between the electron donor and the acceptor, and ε is the dielectric constant of the buffer solutions. Considering that ε of water has a large value and that e^2 is small, the last term in Equation (3) could be neglected in the estimation. The E_{ox} and E_{red} values are the oxidation potentials of **3** and the reduction potentials of **2**. ($E_{ox,3} = 1.01$ V, $E_{red,2} = -0.82$ V; Figure 5). The E_{00} values were calculated from the maximum emission wavelengths of porphyrin **3** (1.95 eV). Therefore, ΔG_{PET} could be calculated as $\Delta G_{PET,2\cdot3} = -0.53$ eV and $\Delta G_{PET,2\cdot4} = -0.87$ eV. The negative ΔG_{PET} value indicated that the PET reaction occurs in a thermodynamically favorable way. It should be noted that because the electrochemical data were non-reversible, there may be errors in the calculation of free-energy changes.

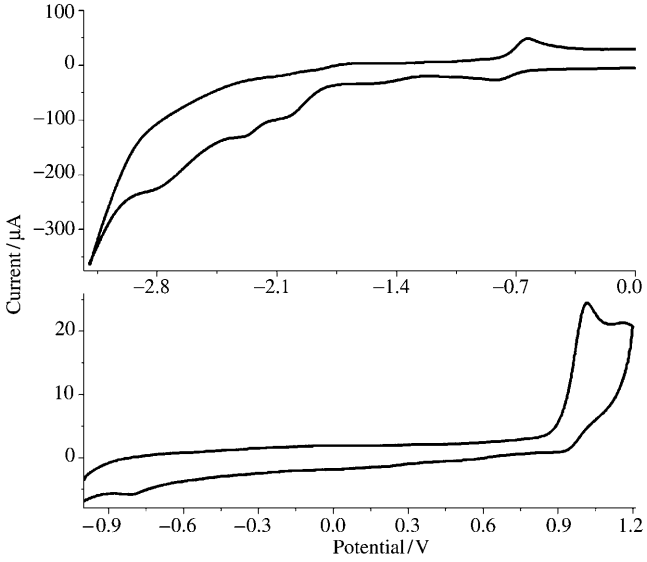

Figure 5. Cyclic voltammogram of **2** (1.5 mM) in THF containing 0.3 M $(tC_4H_9)_4NClO_4$ as the supporting electrolyte (vs. Ag/$AgNO_3$) (top), and **3** (1.0 mM) in aqueous solution containing 0.1 M NaCl as the supporting electrolyte (vs. Ag/AgCl) at 200 mV s^{-1} (bottom).

Nanosecond transient absorption studies: More evidence for the generation of the charge separation (CS) was obtained from the nanosecond transient spectra recorded under the laser irradiation (532 nm). As seen from Figure 6, the absorption peaks corresponding to the excited triplet state of zinc–porphyrin appeared at 620–630 nm and 840 nm.[16] Host

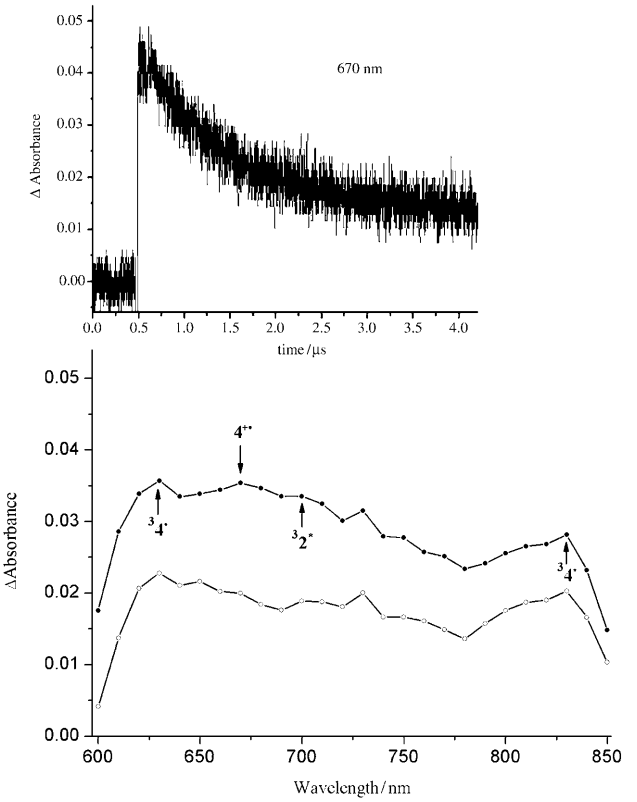

Figure 6. Bottom: Transient absorption spectra of a mixture of **2** (0.2 mM) and **4** (0.2 mM) in ethanol–water–phosphate buffer (v/v = 1:4, pH 7.2) at 180 ns (●) and 1380 ns (○) excited with $\lambda = 532$ nm laser light irradiation at room temperature under N_2-saturated solution. (^{3}**4*** and ^{3}**2*** refer to the centered triplet excited state of **4** and **2**, respectively). Top: Absorption time profile monitored at $\lambda = 670$ nm.

compound **2** showed a band at 700 nm corresponding to the excited triple states. The peak at 670 nm could be assigned to the radical cation of zinc–porphyrin (**4**$^{\bullet+}$). Similarly, in the case of **2·3** system, as a counterpart of the C_{60} radical anion, a shoulder peak at 670 nm in the 300 ns region could be assigned to the radical cation of free-base porphyrin species (**3**$^{\bullet+}$), while the characteristic features of the triple–triple absorption of **2** and **3** appeared at 630 and 780 nm, respectively, generated from the excited singlet state through the intersystem crossing or present as free species[17] (see the Supporting Information). It is reasonable to assume that the decay of the transient absorption bands could be attributed to the charge recombination (CR), which occurred after the formation of a CS state in the host–guest complexes. Thus, the observations mentioned above provided the experimental proof for the electron-transfer fluorescence-quenching mechanism.

Energy-level diagrams: Taking advantage of the oxidation and reduction potentials, the free energy (ΔG_{cs}) of photoinduced electron transfer calculated above, and the reported energies for the singlet and triplet states,[18] the energy levels diagram of the supramolecular architecture could be constructed in Figure 7; these diagrams clearly showed the oc-

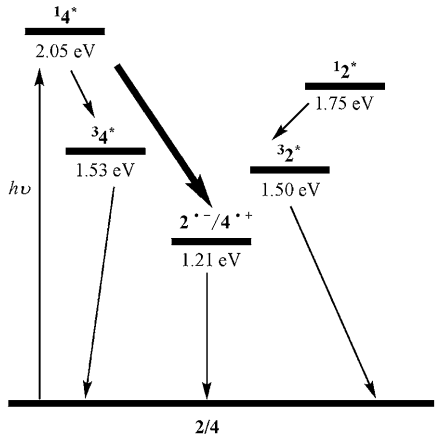

Figure 7. Energy level diagram and electron-transfer paths via excited singlet states of **4**.

currence of sequential electron transfer. It can be seen that there is a much more energetically favorable pathway from the excited singlet states of **4** to the charge-separated state ($\mathbf{2}^{-}/\mathbf{4}^{\bullet+}$) via a host–guest complex. Moreover, as proved by the transient absorption measurement, these metastable species generated from the charge-separated state turned to the ground state through a charge recombination process.

TEM, AFM, and SEM images: The NOESY spectrum of a **2**•**3** system in D_2O/CD_3OD (1:1, v/v; see the Supporting Information) showed that the protons of pyrrole and phenyl group of **3** exhibited NOE correlations with the protons of the secondary -OCH_3 groups of CD cavity. These results indicate that **3** was included in the cavities of **2** from the secondary face, that is, the wide opening. Therefore, transmission electron microscopic (TEM), atomic force microscopic (AFM), and scanning electron microscopic (SEM) experiments were performed to give the visual information about the size and shape of the aggregate. As shown in Figure 8, the TEM image displays the several linear structures with various lengths of more than 200 nm and a similar width of about 2.0 nm (Figure 8a). Furthermore, the AFM images (Figure 8b) present a fine structure of the linear aggregates, which indicated that the linear structure observed in the TEM was actually composed of an ordered single-lined array. The measured average height of the single-lined array is about 2.2 nm, which is basically consistent with TEM image and its length ranges from hundreds of nanometers to micron dimensions. Similarly, a number of square prisms consisting of parallel fiberlike nanowires were also observed in the field of SEM image (Figure 8c), which corresponds to the three-dimensional extension of the single lines in the AFM and TEM images.

Conclusions

A new C_{60}-bridged bis(β-CD) **2** was successfully synthesized by a [1+2] cycloaddition reaction and was fully characterized. The introduction of CD efficiently increased the water solubility of host compounds (up to 1 mM in water). Upon the addition of **2**, the fluorescence of two water-soluble porphyrins (**3** and **4**) quenched dramatically as a result of the PET process between the porphyrins and the C_{60} moiety. Benefiting from the much stronger complexation between **2** and the porphyrins (**3** and **4**), linear supramolecular architectures were successfully constructed. This supramolecular donor/accepter-type architecture offers a new opportunity to transform the PET process to the photovoltaic materials. These findings also suggest that the C_{60}–porphyrin supramolecular dyads and their nanoarchitecture are of special interest in the preparation of devices for the design of novel photovoltaic devices and artificial photosynthetic systems and in the conversion of solar energy. The photovoltaic properties of this fullerene derivative as a donor moiety are currently in progress.

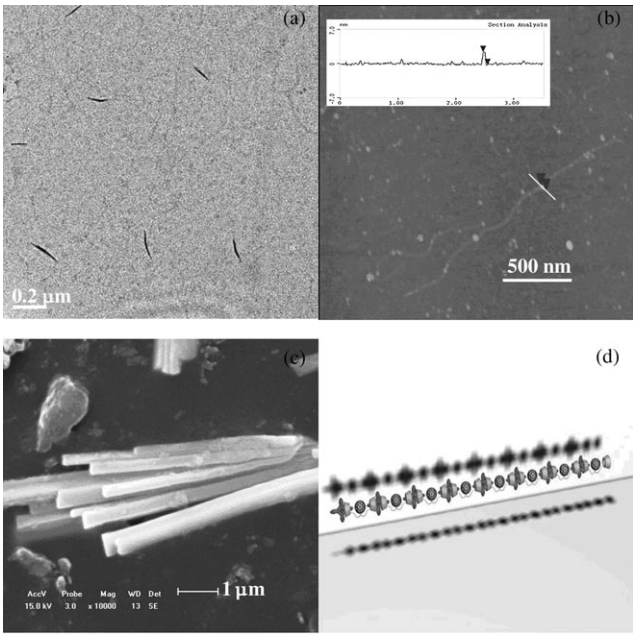

Figure 8. Typical a) TEM, b) AFM, c) SEM images, and d) schematic representation of the linear nanoarchitectures formed by **2** and **3**.

Experimental Section

Instrumentation: Fluorescence spectra were recorded in a conventional quartz cell (10×10×45 mm) at 25 °C on a VARIAN CARY Eclipse spectrometer with the excitation and emission slits of 5 nm widths. Fluorescence lifetimes were measured with an Edinburgh Analytical Instruments FL900CD spectrometer employing the time-correlated single-photon-counting technique. Nanosecond pulsed excitation was carried out with an nF-900 flash lamp filled with ultrapure hydrogen (0.4 bar, 40 kHz repetition rate). No polarizers were used. The signal was detected by a red-sensitive Peltier system cooled S900 single-photon photomultiplier detection system. The chromophores were excited at 414 and 422 nm, and time-resolved fluorescence decays were recorded on a timescale of 100 and 200 ns, resolved into 1024 channels, to a total of 5000 counts in the peak channel by collecting emission at 603 and 642 nm, with a bandwidth of 18 nm. Decay curves were analyzed by using a standard iterative re-

convolution method in the F900 software packages. A multiexponential decay function was assumed [Eq. (4)] in which B_i are pre-exponential factors, τ_i are the characteristic lifetimes, and A is an additional background factor.

$$R(t) = A + \sum_{i=1}^{4} B_i e^{-t/\tau_i} \quad (4)$$

Nanosecond transient absorption spectra were performed on a LP-920 pump-probe spectroscopic setup. The excited source was the unfocused third harmonic 532 nm output of a Nd:YAG laser (10 Hz, 8 ns; Continuum surelite II); the probe light source was a pulse-xenon lamp. The signals were detected by Edinburgh analytical instruments (LP900) and recorded on a Tektronix TDS 3012B oscilloscope and a computer. Elemental analyses were performed on a Perkin–Elmer-2400C instrument. NMR spectra were recorded on Bruker AV300 and Varian Mercury Plus 400 instruments. UV/Vis spectra were recorded in a conventional quartz cell (light path 10 mm) on a Shimadzu UV-2401PC spectrophotometer equipped with a PTC-348WI temperature controller to keep the temperature at 25 °C. The cyclic voltammetry (CV) measurements were carried out on a BAS Epsilon electrochemical analyzer with C3 cell stand. At the beginning of the electrochemistry experiment, the aqueous solution was deoxygenated by purging with dry nitrogen for at least 15 min. All the solutions were prepared in deionized water at 298 K containing 0.1 M NaCl or in dry THF containing $(t\mathrm{C_4H_9})_4\mathrm{NClO_4}$ as a supporting electrolyte $(200\ \mathrm{mV\,s})^{-1}$. The glassy carbon working electrode was polished with 0.05 μm BAS alumina suspension on a brown Texmet polishing pad, sonicated in distilled water for a few minutes to remove any residual alumina particles, and then rinsed with ethanol before use. A platinum wire was used as the counter electrode. The measured potentials were recorded with respect to an Ag/AgCl (immersed in a solution containing 3 M sodium chloride) or $Ag/AgNO_3$ reference electrode. In AFM measurements, a drop of sample solution (1.0×10^{-6} M) was dropped onto newly clipped mica and then air-dried, which was examined using an AFM (Veeco Company, Multimode, Nano IIIa) in tapping mode in the air at room temperature. Transmission electron microscopy (TEM) experiments were performed using a Philips Tacnai G^2 20 S-TWIN microscope operating at 200 kV. TEM samples (1.0×10^{-6} M) were prepared by depositing a drop of the suspension onto a holey carbon grid or by placing a drop of the solution onto a carbon coated copper grid. SEM images were recorded on a HITACHI S-3500N scanning electron microscope.

Materials: All the chemicals were used as reagent grade unless noted. Propargyl alcohol, sodium ascorbate and 5,10,15,20-tetrakis(4-sulfonatophenyl)porphyrin (**3**) were purchased from commercial resources and used as received. β-CD was recrystallized twice from water and dried in vacuo at 90 °C for 24 h. 6-Deoxy-6-azido-permethyl-β-CD,[19] propargyl malonate[20] and **4**[21] were prepared according to the literature procedure. Column chromatography was performed on 200–300 mesh silica gels.

Bis{4-methyl[1,2,3]triazolyl}malonic ester-bridged bis(permethyl-β-CD) 1: $CuSO_4{\cdot}5H_2O$ (392.6 mg) dissolved in water (50 mL) was added to a solution of propargyl malonate (0.26 mmol, 47.2 mg) and 6-deoxyl-6-azido-permethyl-β-CD (1.1 g, 0.79 mmol) in THF (15 mL). The mixture was kept at 50 °C for 10 min, then sodium ascorbate (777.3 mg) was added. The color of the mixture immediately turned brown and then dark purple after a few minutes. The mixture was heated at 50 °C for 12 h. After cooling to room temperature, the brown-yellow solution was dried under reduced pressure, and the residue was dissolved in chloroform (50 mL). Insoluble precipitates were removed by filtration, and the filtrates were evaporated in vacuo and further purified by flash column chromatography using $CHCl_3/CH_3OH$ (100:3, v/v) as eluent to give the product as a white powder in 70% yield. ^{1}H NMR (400 MHz, $CDCl_3$): $\delta=3.02$–3.95 (m, 206H), 5.05–5.20 (m, 14H), 5.22–5.32 (m, 4H), 7.73 ppm (s, 2H); ^{13}C NMR (75 MHz, $CDCl_3$): $\delta=29.8$, 41.1, 51.4, 58.7, 59.1, 61.5, 71.1, 71.4, 77.6, 79.1, 80.4, 81.9, 82.2, 98.3, 99.0, 126.3, 141.6, 166.2 ppm; elemental analysis calcd (%) for $C_{133}H_{226}N_6O_{72}$: C 52.18, H 7.44, N 2.75; found: C 51.90, H 7.64, N 2.71; MALDI-MS: m/z: 3061 $[M+H]^+$, 3083 $[M+Na]^+$.

1,1-Fullerene-bis{4-methyl[1,2,3]triazolyl}malonic ester-bridged bis(permethyl-β-CD) 2: A solution of **1** (430.4 mg, 0.13 mmol) in dry DMF (42 mL) was added to a solution containing C_{60} (101.3 mg, 0.12 mmol) and CBr_4 (33.2 mg, 0.1 mmol) in dry toluene (110 mL). The reaction mixture was stirred at room temperature in the dark for 24 h. Then, 1,8-diaza-bicyclo[5.4.0]undec-7-ene (DBU, 22.3 μL) in toluene (10 mL) was added dropwise to the mixture under nitrogen. After the mixture was stirred for an additional 1 day at room temperature, the deep purple homogeneous solution turned deep brown. The solution was dried in vacuo, and the residue was dissolved in chloroform. After the removal of insoluble salts by filtration, the filtrate was extracted with water for three times. Then, the mixture was concentrated and purified by silica gel column chromatography eluting with $CHCl_3$ and $CHCl_3/CH_3OH$ (200:3, v/v) to give **2** (196 mg, yield 37%) as a dark brown solid. ($R_f=0.3$). ^{1}H NMR (400 MHz, $CDCl_3$): $\delta=3.18$–3.88 (m, 204H), 5.02–5.24 (m, 12H), 5.28–5.39 (m, 2H), 5.51–5.67 (m, 4H), 7.89 ppm (s, 2H); ^{13}C NMR (75 MHz, $CDCl_3$): $\delta=29.9$, 51.4, 58.5, 58.7, 58.8, 59.2, 59.5, 60.5, 61.5, 61.9, 70.4, 71.2, 71.6, 77.5, 79.0, 79.9, 80.1, 80.5, 80.6, 81.3, 81.7, 82.0, 82.2, 82.4, 98.4, 98.9, 99.4, 127.0, 139.2, 141.2, 141.9, 142.3, 143.1, 143.2, 144.1, 144.6, 144.8, 145.1, 145.2, 145.5, 163.5. ppm; elemental analysis calcd (%) for $C_{193}H_{224}N_6O_{72}$: C 61.33, H 5.97, N 2.22; found: C 61.63, H 5.77, N 2.40; MALDI-MS: m/z: 3802 $[M+Na]^+$.

Acknowledgements

We thank 973 Program (2006CB932900), NNSFC (20721062 and 20772062), Tianjin Natural Science Foundation (07QTPTJC29600) and Key Project of Chinese Ministry of Education (No 107026) for financial support.

[1] M. D. Ward, *Chem. Soc. Rev.* **1997**, *26*, 365–375.
[2] H. Spanggaard, C. Frederik, F. C. Krebs, *Sol. Energy Mater. Sol. Cells* **2004**, *83*, 125–146.
[3] a) P. A. Liddell, G. Kodis, L. Garza, J. L. Bahr, A. L. Moore, T. A. Moore, D. Gust, *Helv. Chim. Acta* **2001**, *84*, 2765–2783; b) S. Saha, E. Johansson, A. H. Flood, H. Tseng, J. I. Zink, J. F. Stoddart, *Chem. Eur. J.* **2005**, *11*, 6846–6858.
[4] a) L. Sánchez, N. Martín, D. M. Guldi, *Angew. Chem.* **2005**, *117*, 5508–5516; *Angew. Chem. Int. Ed.* **2005**, *44*, 5374–5382; b) M. Morisue, S. Yamatsu, N. Haruta, Y. Kobuke, *Chem. Eur. J.* **2005**, *11*, 5563–5574.
[5] N. Martin, F. Giacalone, J. L. Segura, D. M. Guldi, *Synth. Met.* **2004**, *147*, 57–61.
[6] a) A. S. D. Sandanayaka, Y. Araki, O. Ito, R. Chitta, S. Gadde, F. D'Souza, *Chem. Commun.* **2006**, 4327–4329; b) T. Hasobe, P. V. Kamat, M. A. Absalom, Y. Kashiwagi, J. Sly, M. J. Crossley, K. Hosomizu, H. Imahori, S. Fukuzumi, *J. Phys. Chem. B* **2004**, *108*, 12865–12872; c) L. Valentini, M. Trentini, F. Mengoni, J. Alongi, I. Armentano, L. Ricco, A. Mariani, J. M. Kenny, *Diamond Relat. Mater.* **2007**, *16*, 658–663; d) J. Hou, H. Yi, X. Shao, C. Li, Z. Wu, X. Jiang, L. Wu, C. Tung, Z. Li, *Angew. Chem.* **2006**, *118*, 810–814; *Angew. Chem. Int. Ed.* **2006**, *45*, 796–800.
[7] L. Dai, A. H. Mau, *Adv. Mater.* **2001**, *13*, 899–913.
[8] a) A. Cravino, *Polym. Int.* **2007**, *56*, 943—956; b) A. Cravino, N. S. Sariciftci, *J. Mater. Chem.* **2002**, *12*, 1931–1943; c) Z. Liang, K. L. Dzienis, J. Xu, Q. Wang, *Adv. Funct. Mater.* **2006**, *16*, 542–548; d) G. Tu, H. Li, M. Forster, R. Heiderhoff, L. J. Balk, U. Scherf, *Macromolecules* **2006**, *39*, 4327–4331.
[9] a) K. Kano, H. Kitagishi, S. Tamura, A. Yamada, *J. Am. Chem. Soc.* **2004**, *126*, 15202–15210; b) K. Kano, H. Kitagishi, C. Dagallier, M. Kodera, T. Matsuo, T. Hayashi, Y. Hisaeda, S. Hirota, *Inorg. Chem.* **2006**, *45*, 4448–4460.
[10] a) S. Filippone, A. Rassat, *C. R. Chim.* **2003**, *6*, 83–86; b) S. Filippone, F. Heimann, A. Rassat, *Chem. Commun.* **2002**, 1508–1509;

c) J. Yang, Y. Wang, A. Rassat, Y. Zhang, P. Sinay, *Tetrahedron* **2004**, *60*, 12163–12168.

[11] a) Y. Zhao, L. Wu, G. Si, Y. Liu, H. Xue, L. Zhang, C. Tung, *J. Org. Chem.* **2007**, *72*, 3632–3639; b) H. Kim, J. Heo, W. S. Jeon, E. Lee, J. Kim, S. Sakamoto, K. Yamaguchi, K. Kim, *Angew. Chem.* **2001**, *113*, 1574–1577; *Angew. Chem. Int. Ed.* **2001**, *40*, 1526–1529.

[12] a) T. Hasobe, H. Imahori, P. V. Kamat, T. K. Ahn, S. K. Kim, D. Kim, A. Fujimoto, T. Hirakawa, S. Fukuzumi, *J. Am. Chem. Soc.* **2005**, *127*, 1216–1228; b) B. Valeur, *Molecular Fluorescence: Principles and Applications*, Wiley-VCH, Weinheim, **2002**; c) N. Tomioka, D. Takasu, T. Takahasahi, T. Aida, *Angew. Chem.* **1998**, *110*, 1611–1614; *Angew. Chem. Int. Ed.* **1998**, *37*, 1531–1534.

[13] a) A. Kira, T. Umeyama, Y. Matano, K. Yoshida, S. Isoda, J. K. Park, D. Kim, H. Imahori, *J. Am. Chem. Soc.* **2009**, *131*, 3198–3200; b) Y. Kuramochi, A. S. D. Sandanayaka, A. Satake, Y. Araki, K. Ogawa, O. Ito, Y. Kobuke, *Chem. Eur. J.* **2009**, *15*, 2317–2327.

[14] a) C. Ehli, G. M. A. Rahman, N. Jux, D. Balbinot, D. M. Guldi, F. Paolucci, M. Marcaccio, D. Paolucci, M. Melle-Franco, F. Zerbetto, S. Campidelli, M. Prato, *J. Am. Chem. Soc.* **2006**, *128*, 11222–11231; b) R. Chitta, A. S. D. Sandanayaka, A. L. Schumacher, L. D'Souza, Y. Araki, O. Ito, F. D'Souza, *J. Phys. Chem. C* **2007**, *111*, 6947–6955; c) P. Liang, H. Zhang, Z. Yu, Y. Liu, *J. Org. Chem.* **2008**, *73*, 2163–2168.

[15] a) G. H. Sarova, U. Hartnagel, D. Balbinot, S. Sali, N. Jux, A. Hirsch, D. M. Guldi, *Chem. Eur. J.* **2008**, *14*, 3137–3145; b) Y. Kuramochi, A. Satake, M. Itou, K. Ogawa, Y. Araki, O. Ito, Y. Kobuke, *Chem. Eur. J.* **2008**, *14*, 2827–2841; c) F. D'Souza, E. Maligaspe, P. A. Karr, A. L. Schumacher, M. E. Ojaimi, C. P. Gros, J. Barbe, K. Ohkubo, S. Fukuzumi, *Chem. Eur. J.* **2008**, *14*, 674–681; d) D. Bonifazi, A. Kiebele, M. Stöhr, F. Cheng, T. Jung, F. Diederich, H. Spillmann, *Adv. Funct. Mater.* **2007**, *17*, 1051–1062; e) L. Sánchez, M. Sierra, N. Martín, A. J. Myles, T. J. Dale, J. Rebek, Jr., W. Seitz, D. M. Guldi, *Angew. Chem.* **2006**, *118*, 4753–4757; *Angew. Chem. Int. Ed.* **2006**, *45*, 4637–4641.

[16] a) A. G. Skillman, J. R. Collins, G. H. Loew, *J. Am. Chem. Soc.* **1992**, *114*, 9538–9544; b) M. Fujitsuka, O. Ito, T. Yamashiro, Y. Aso, T. Otsubo, *J. Phys. Chem. A* **2000**, *104*, 4876–4881; c) F. D'Souza, R. Chitta, S. Gadde, A. L. McCarty, P. A. Karr, M. E. Zandler, A. S. D. Sandanayaka, Y. Araki, O. Ito, *J. Phys. Chem. B* **2006**, *110*, 5905–5913.

[17] a) T. Hasobe, A. S. D. Sandanayaka, T. Wada, Y. Arakic, *Chem. Commun.* **2008**, 3372–3374; b) F. D'Souza, P. M. Smith, M. E. Zandler, A. L. McCarty, M. Itou, Y. Araki, O. Ito, *J. Am. Chem. Soc.* **2004**, *126*, 7898–7907.

[18] a) S. Komamine, M. Fujitsuka, O. Ito, K. Morikawa, K. Miyata, T. J. Ohno, *J. Phys. Chem. A* **2000**, *104*, 11497–11504; b) M. Yamazaki, Y. Araki, M. Fujitsuka, O. Ito, *J. Phys. Chem. A* **2001**, *105*, 8615–8622; c) F. D'Souza, S. Gadde, M .E. Zandler, K. Arkady, M. E. El-Khouly, M. Fujitsuka, O. Ito, *J. Phys. Chem. A* **2002**, *106*, 12393–12404; d) F. D'Souza, S. Gadde, A. L. Schumacher, M. E. Zandler, A. S. D. Sandanayaka, Y. Araki, O. Ito, *J. Phys. Chem. C* **2007**, *111*, 11123–11130.

[19] a) C. Hocquelet, J. Blu, C. K. Jankowski, S. Arseneau, D. Buisson, L. Mauclaire, *Tetrahedron* **2006**, *62*, 11963–11971; b) M. T. Reetz, S. R. Waldvogel, *Angew. Chem.* **1997**, *109*, 870–873; *Angew. Chem. Int. Ed. Engl.* **1997**, *36*, 865–867.

[20] Y. Zhang, B. Hu, C. Xia, Z. Chen, Y. Yin, *Chin. J. Synth. Chem.* **2002**, *10*, 335–337.

[21] a) C. M. N. Azevedo, K. Araki, L. Angnes, H. E. Toma, *Electroanalysis* **1998**, *10*, 467–471; b) C. M. N. Azevedo, K. Araki, H. E. Toma, L. Angnes, *Anal. Chim. Acta* **1999**, *387*, 175–180.

Received: June 16, 2009
Published online: September 16, 2009

